PHYSICAL REVIEW B VOLUME 36, NUMBER 9 15 SEPTEMBER 1987-II

Ionic and superionic conductivities of SrF_2 crystals in a wide frequency range

G. A. Evangelakis and Demitrios Miliotis
Department of Physics, University of Ioannina, Ioannina 45332, Greece
(Received 25 March 1987)

The ionic and superionic conductivities of SrF_2 single crystals purchased from Harshaw have been measured at different temperatures as a function of frequency. The temperature varied from 400 to 1010 °C and the frequency ranged from 10 Hz to 10 MHz. We used a coaxial-line configuration, with polished platinum electrodes welded on stainless steel. At all temperatures the apparent conductivity of the sample depended upon the crystal thickness and the measuring frequency. An analysis has been made using complex-impedance diagrams, which led to the conclusion that the actual conductivity is frequency independent in this temperature range. The observed frequency dependence is attributed to poor contact between the crystal and the electrodes, and this is supported by a model analysis based on an equivalent electric circuit with air-gap capacitance. Therefore no frequency dependence can be deduced for the conductivity of SrF_2 crystals. In addition, from the experimental Arrhenius diagram, we calculate extrinsic and intrinsic enthalpies.

I. INTRODUCTION

Crystals with fluorite structure have been the subject of a great deal of study in recent years. The nature of the high values of the ionic conductivity of these superionic conductors, the sometimes conflicting results of the experiments, but mainly the lack of data for the superionic conductivity over a wide frequency range, were some of the underlying reasons that convinced us to conduct this experiment. In this paper we concentrate our attention on a single material SrF_2, and explore the frequency dependence of the conductivity in the ionic and superionic states. We tried as well to detect the absorption band, if any, due to reorientation of Debye dipoles as a function of frequency. Consequently we divided the whole temperature range into two parts, one from 400 to 700 °C and the other from 700 to 1010 °C. In the low-temperature range, we thought that we would overcome the electrode problem[1-3] by leaving the crystal at a constant temperature until the slope of the straight line $\ln(\epsilon_2)$ versus $\ln(f)$ became -1. However we did not succeed in obtaining a slope of -1, and all the data in the present work, as far as the ionic phase of the crystal is concerned, were taken with slopes ranging between -0.97 to -0.99, a fact which indicates that the electrode problem was always present. Nevertheless, some results concerning the activation enthalpies have emerged from the present work. It should be pointed out that, in the low-temperature regime, the absolute value of the slope was monotonically increasing as a function of time, while in the high-temperature regime we observed an increase at first, followed by a temporary saturation and then by a decrease, which is attributed to the evaporation of the fluorine from the SrF_2 crystal.

II. EXPERIMENT

All the samples used were single crystals purchased from Harshaw. They were cut along planes normal to the [111] direction and polished on both sides with different kinds of abrasive paper. The samples used were of different thicknesses and cross-sectional areas. The resistance of the different samples of SrF_2 was measured at temperatures ranging from 400 to 1010 °C and at frequencies between 10 Hz and 10 MHz. Each sample was set on platinum electrodes welded on stainless steel, which comprised the coaxial line described elsewhere.[4] The coaxial line was inside an ohmic furnace with a voltage-regulated power supply. Temperatures were measured by means of two calibrated Pt–Pt + 10% Rh thermocouples, connected to a digital thermometer of multiple inputs and in parallel with a two-input recorder. All measurements were taken in a commercially pure inert-gas (Ar) atmosphere, which was further purified by passing it over hot Ti chips in order to eliminate the possible presence of oxygen. The stability of the sample's temperature was ensured by (1) the stabilized heating power for the furnace and (2) the high thermocapacity of the coaxial line, a part of which was a stainless-steel cylinder, 1.2 cm high and with a diameter of 4.6 cm.

Sample resistances and capacitances were measured with (i) a General Radio 1621 precision capacitance measurement system (range 10 Hz–100 kHz) (ii) a Boonton 75-C direct capacitance bridge (range 5–500 kHz and (iii) a Hewlett-Packard 4275A multifrequency *LCR* meter (range 10 kHz–10 MHz). The Boonton 75-C capacitance bridge, was used for cross checking the region where the ranges of systems (i) and (iii), had a poor frequency overlap.

For each sample, at constant temperature and frequency, the input voltage was varied, but none of the measured physical quantities showed any significant dependence. We measured the conductance for a number of samples of different sizes, at the same frequency and temperature. The values for the conductance were found to be different for each sample, indicating the

presence of the Maxwell-Wagner polarization. We measured also the conductance as a function of time at constant frequency and temperature and we observed a time dependence. In particular in the low-temperature range (400 °C to 700 °C), we found an average increase of 1% per hour for the conductivity over a period of six hours, followed by saturation in the next couple of hours. In the high-temperature range (700 to 1010 °C) we observed an average increase of 2.5% per hour in the conductivity over a period of two hours, followed by a decrease.

In the low-temperature range the contact between the crystal and the electrodes improved with time, failing, however, to become absolutely perfect. In the high-temperature range initially we observed the same behavior as in the low-temperature range, but subsequently the evaporation of the fluorine created a layer of gas which played the role of an air gap[1] that reduced the conductance. After cooling the crystal we were able to observe, on the electrodes, a mosaic of both shiny and dimly reflecting patches. The latter corresponds to the regions where the crystal was in good contact with the electrodes.

III. RESULTS AND DISCUSION

The conductivity measurements are shown in Figs. 1 and 2 along with their associated error bars. All measurements have been taken when the conductance reached a saturation value, for the low-temperature range, and when the conductance reached its maximum, for the high-temperature range.

A. Frequency dependence of the conductivity

The conductivity of SrF_2, as calculated from raw data and displayed in Fig. 1, showed a clear frequency dependence and a dispersion peak which could be attributed to the reorientation of Debye-type dipoles. The position of the maximum of this peak is shifted to higher frequencies as the temperature increases, following the relation

$$f = f_0 \exp\left[-\frac{E}{kT}\right],$$

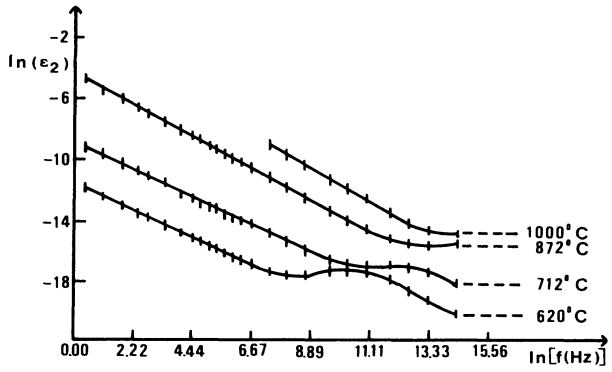

FIG. 1. The logarithm of the imaginary part of the dielectric constant vs the logarithm of the frequency at various temperatures.

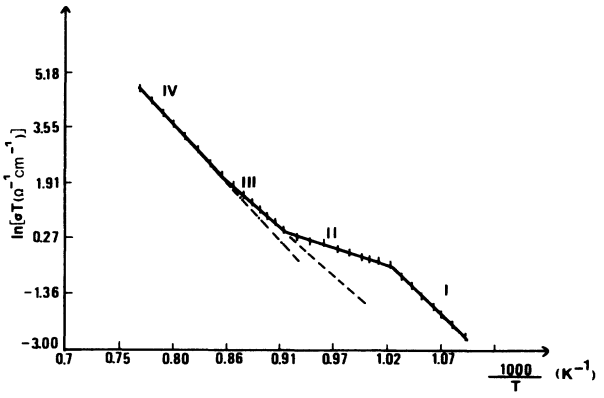

FIG. 2. Conductivity dependence upon temperature.

where f is the peak frequency, f_0 is the Debye limiting frequency, E is the energy required for the reorientation process, k is Bolltzman's constant, and T is the absolute temperature. From this temperature dependence an activation energy of the order of 0.2 eV is deduced.

Collectively the curves in Fig. 1 can be described quite accurately by the functional form

$$\sigma = A \exp\left[-\frac{(f-B)^2}{C}\right] + Df + E ,$$

where A, B, C, D, and E are constants, while σ and f stand for the conductivity and the frequency, respectively. The values for the constants were determined by a least-squares fit to the experimental data. This was facilitated by use of the program MERLIN for multidimensional nonlinear optimization.[5] The Gaussian term corresponds to the Debye-dipole-reorientation-induced conductivity and the other two terms correspond to dc conductivity. This however is not an intrinsic property of the crystal; it is attributed to the poor electrode-crystal contacts, as discussed below.

Since the apparent conductivity was found to be both time and size dependent, complex-impedance diagrams are proper, as suggested[2,6] and used by others.[3] Two plots of this kind are shown in Fig. 3 from which the bulk resistances of the crystal R_{∞_1} and R_{∞_2}, can be calculated. This kind of plot[3] corresponds to the electric circuits shown in Figs. 4(a) and 4(b).[7]

Assuming that the crystal has both regions of good-quality contacts with the electrodes and regions of poor contacts due to creation of air gaps between the crystal and the electrodes, we model our analysis as follows. The good-quality-contact part of the crystal-electrode system, can be described by an equivalent circuit that consists of a capacitance C_1 and a resistance R_1 in parallel. In Fig. 4 C_1 and R_1 correspond to the geometrical capacitance and to the bulk resistance, respectively, of the sample for which the electrode contact is good. The effect of imperfect electrode contact at the remaining part of the sample can be described by a resistance R_b in series with a capacitance C_b. Again R_b corresponds to the bulk resistance of the part in question, while C_b results from the existence of the contact-

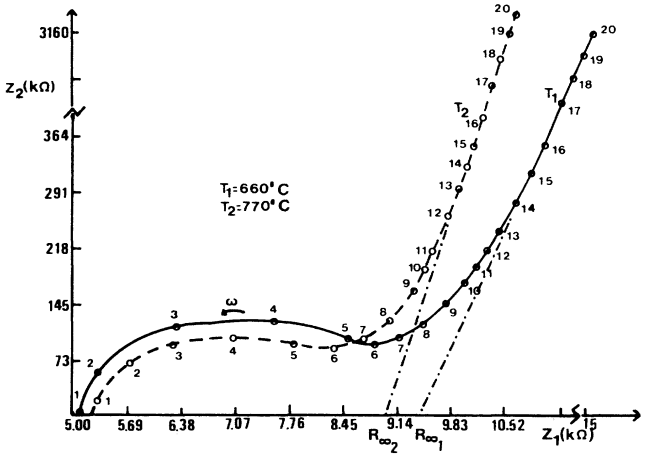

FIG. 3. The complex-impedance diagram at two different temperatures. The points numbered from 1 to 20 correspond to frequencies: 10 MHz, 4 MHz, 2 MHz, 1 MHz, 400 kHz, 200 kHz, 100 kHz, 40 kHz, 20 kHz, 10 kHz, 5 kHz, 2.5 kHz, 1.2 kHz, 1 kHz, 0.8 kHz, 0.4 kHz, 0.18 kHz, 80 Hz, 20 Hz, 10 Hz.

spoiling air gaps.

The equivalent Voigt model with the Warburg admittance V_W in Fig. 4(b) permits us to calculate the bulk resistance $R_\infty \approx R_1$ of the crystal, from the complex-impedance plot. We found that the Warburg admittance is a function of time and temperature,[8] in agreement with other[3] experiments. This corresponds to slope values closer to -1 in the $\ln\epsilon_2$ versus $\ln f$ plot and to a shift of the peak to higher frequencies with rising temperatures. The latter can be attributed to the fact that at higher temperatures C_b and R_b show a tendency to disappear since then the contact between the electrodes and the crystal becomes better. The graphs of the complex impedance corresponding to the electric circuit of Fig. 4(b), are shown in 4(c). These graphs have the form of our experimental curves, leading to the conclusion that the apparent frequency dependence of the conductivity is not an intrinsic property of the material but is due to the imperfect nature of the crystal-electrode contact.

B. Temperature dependence of the conductivity

In Fig. 2 the conductivity of SrF_2 as a function of the temperature is shown. This is a typical Arrhenius plot, similar to those found for other alkaline-earth halides.

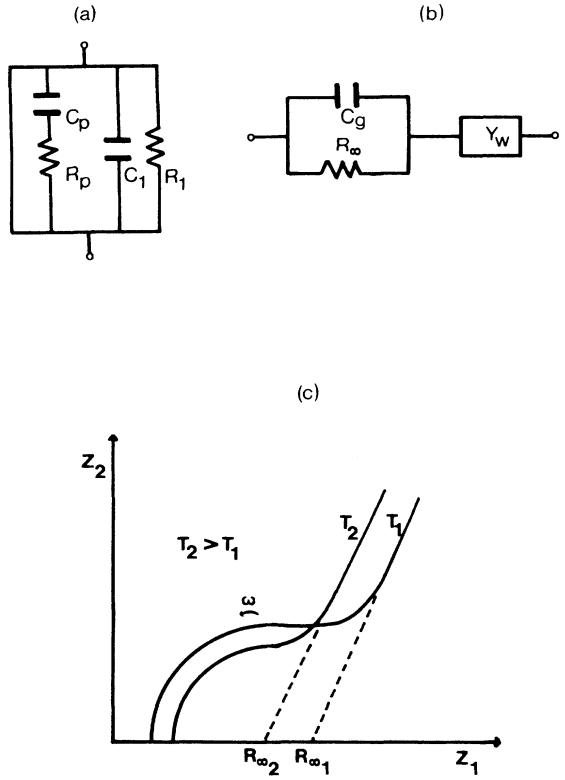

FIG. 4. (a) The assumed equivalent circuit for the crystal-electrodes systems. (b) The equivalent Voigt model. (c) Complex-impedance graph for the adopted equivalent circuit.

The conductivity values indicated there, are taken from the complex-impedance diagrams of the raw data. In this figure we distinguish four different regions, each represented by a straight line, that characterize the different mechanisms of conduction.

Each region, can be represented by an expression of the form

$$\ln(\sigma T)=\ln\sigma_0-\frac{H}{kT}\ , \tag{1}$$

where σ is the conductivity, H is the activation enthalpy, k is Boltzmann's constant, and T is the absolute temperature. For each region of interest, σ_0 is determined in what follows.

For a pure ionic conductor with one carrier present,

$$\sigma=qn\mu\ , \tag{2}$$

TABLE I. Values of activation enthalpies and preexponential factors determined by the present work, along with the corresponding values found by others.

H^m (eV)	H^F (eV)	H_{intr} (eV)	σ_0(intr)	References
0.94	1.74	1.81	2.5×10^8	13, 16
1.0	2.28	2.14±0.03	5.6×10^9	1
0.96±0.04	2.28±0.11	2.1±0.08	5.8×10^9	15
0.43	2.38	1.93		17
1.04±0.04	2.0±0.08	2.04±0.08	2.2×10^9	Present work

where q is the charge, n is the number, and μ the mobility of the carrier (i.e., q_v, n_v, μ_v for vacancies and q_i, n_i, μ_i for interstitials). Generally the mobility is given by the equation

$$\mu = \frac{\lambda \omega q}{kT} \exp\left[-\frac{\Delta G^m}{kT} \right], \tag{3}$$

where ω is the attempt frequency, λ is a geometrical factor, and ΔG^m is the free energy required for migration.

At intermediate temperatures, in region II, called the extrinsic disassociation region, the number of defects (vacancies or interstitials) is temperature independent. The existence of such a region is due to defects introduced by the presence of aliovalent impurities,[9,10] which are always present even in pure crystals. Thus, in our case, trivalent cations, if any, would introduce interstitials, while monovalent cations would introduce vacancies. We believe that the behavior in region II is mainly due to the motion of vacancies introduced by the oxygen contamination of the sample and thus the activation enthalpy H_{II} can be ascribed to the migration enthalpy of the vacancies H^m. We think so because (i) as time went by, the sample's conductivity increased and (ii) samples that were preheated at high temperatures and thus contaminated with oxygen, displayed higher conductivity. The formation of these vacancies can be justified by considering that a divalent oxygen anion can replace two monovalent fluorines, leaving one anionic site vacant.

So for region II, combining Eqs. (1)–(3) and the relation

$$\Delta G = \Delta H - T\Delta S \tag{4}$$

with ΔH and ΔS the enthalpy and the entropy difference, respectively, we obtain

$$\sigma_0 = \frac{q_v^2 n \lambda \omega}{k} \exp\left[\frac{\Delta S^m}{k} \right] \exp\left[\frac{\Delta S^v}{k} \right], \tag{5}$$

where ΔS^m and ΔS^v stand for the entropy for migration and formation of vacancies, respectively, and n is their number. At even lower temperatures association between the aliovalent impurities and the compensating defect becomes almost complete and we obtain region I called the extrinsic association region.

As the temperature is increased, we enter region III, where the conductivity is an intrinsic property of the crystal. For this region, it is well known that for crystals with the fluorite structure the defects are mainly *anti-Frenkel* type.[9,11,12] This implies that at high temperatures like those of region III, the number of vacancies is equal to the number of interstitials. The slope of the straight line in region III of Fig. 2, is taken to be the intrinsic enthalpy H_{intr}. Recalling that the density of the anti-Frenkel defects is given by

$$n^F = \sqrt{NN_0} \exp\left[-\frac{\Delta G^F}{kT} \right], \tag{6}$$

where N is the number of mobile ions per unit volume, N_0 is the number of available interstitial sites, and ΔG^F is the Gibb's-energy difference, and using relations (1)–(4) and (6), σ_0 can be expressed as

$$\sigma_0 = \frac{q^2 \lambda \omega \sqrt{N_0 N}}{k} \exp\left[\frac{\Delta S^m}{k} \right] \exp\left[\frac{\Delta S^F}{2k} \right], \tag{7}$$

where ΔS^F stands for the formation entropy of the anti-Frenkel defect.

The formation enthalpy H^F of the anti-Frenkel defect, can be calculated from

$$H_{\text{intr}} = H^m + \tfrac{1}{2} H^F . \tag{8}$$

As the temperature is further increased we observe an additional increase of the conductivity (region IV of the Arrhenius-type diagram). We attribute this increase to the migration of an interstitial ion to a lattice or to an interstitial site[13,14] and to possible contamination of the crystal by oxygen.[13,15]

In Table I values of the various physical quantities as determined in this work are shown along with the corresponding values found by others.

ACKNOWLEDGMENTS

Thanks are due to Mr. N. Vasos of Coordinated Science Laboratory of the University of Illinois for the elegant work concerning the welding of Pt electrodes on stainless steel. The authors also thank Dr. G. Giakoumakis for his help in constructing the experimental apparatus, and Dr. I. E. Lagaris for constructive criticism.

[1] D. Miliotis and D. N. Yoon, J. Phys. Chem. Solids **30**, 1241 (1969).
[2] J. R. Macdonald, J. Chem. Phys. **58**, 4982 (1973).
[3] A. D. Reed and D. Lazarus, Phys. Rev. B **27**, 6504 (1983).
[4] E. Barsis and A. Taylor, J. Chem. Phys. **45**, 1145 (1966). (1966).
[5] G. A. Evangelakis, J. P. Rizos, I. E. Lagaris, and I. N. Demetropoulos, Comp. Phys. Commun. (to be published).
[6] J. R. Macdonald, J. Chem. Phys. **60**, 343 (1973).
[7] J. R. Macdonald, in *Superionic Conductors,* edited by G. Mahan and W. Roth (Plenum, New York, 1976).
[8] J. R. Macdonald, J. Chem. Phys. **61**, 3977 (1974).
[9] A. B. Lidiard, in *Electrical Conductivity,* Vol. 20 of Encyclopedia of Physics, edited by S. Flugge (Springer, Berlin, 1957).
[10] P. Suptitz and J. Teltow, Phys. Status Solidi **23**, 9 (1967).
[11] A. B. Lidiard, in *Crystal with the Fluorite Structure,* edited by W. Hayes (Oxford University, New York, 1974).
[12] *Superionic Solids,* edited by S. Chandra, (North Holland, Amsterdam, 1981).
[13] W. Bollmann, P. Gorlich, W. Hauk, and H. Mothes, Phys. Status Solidi **2**, 157 (1970).
[14] A. B. Lidiard, Nuovo Cimento Suppl. **7**, 620 (1958).
[15] J. Oberschmidt and D. Lazarus, Phys. Rev. B **21**, 5823 (1980).
[16] R. W. Bonne and J. Schoonman, J. Electrochem. Soc. **124**, 28 (1977).
[17] C. R. A. Catlow, M. J. Norgett, and T. A. Ross, J. Phys. C **10**, 1627 (1977).